Carbon 161 (2020) 219–223

Contents lists available at ScienceDirect

Carbon

journal homepage: www.elsevier.com/locate/carbon

Strain-controlled magnetic ordering in 2D carbon metamaterials

Dan Liu [a], Eunja Kim [b], Philippe F. Weck [c], David Tománek [a, *]

[a] Physics and Astronomy Department, Michigan State University, East Lansing, MI, 48824, USA
[b] Department of Physics and Astronomy, University of Nevada Las Vegas, Las Vegas, NV, 89154, USA
[c] Sandia National Laboratories, P.O. Box 5800, Albuquerque, NM, 87185, USA

ARTICLE INFO

Article history:
Received 20 December 2019
Received in revised form
16 January 2020
Accepted 17 January 2020
Available online 24 January 2020

Keywords:
Graphene
Carbon
Metamaterial
Magnetism
DFT

ABSTRACT

We use *ab initio* spin-polarized density functional theory to study the magnetic order in a Kagomé-like 2D metamaterial consisting of pristine or substitutionally doped phenalenyl radicals polymerized into a nanoporous, graphene-like structure. In this and in a larger class of related structures, the constituent polyaromatic hydrocarbon molecules can be considered as quantum dots that may carry a net magnetic moment. The structure of this porous system and the coupling between the quantum dots may be changed significantly by applying moderate strain, thus allowing to control the magnetic order and the underlying electronic structure.

1. Introduction

Metamaterials are systems where the separation between the macrostructure and the constituent material has been washed out to gain new functionality. 2D metamaterials with selected nanostructured components can exhibit remarkable mechanical, transport, optical, and electromagnetic properties [1–4]. Whereas isolated constituent nanostructures should be considered as quantum dots, aggregates of such nanostructures may display intriguing physical behavior. Selected 2D metamaterials consisting of graphitic nanostructures, sometimes called “nanoporous graphene”, have been synthesized [5–7] and could find their use in hydrogen storage, gas separation and purification, DNA sequencing, and as magnets and supercapacitors [8,9]. One of such graphitic nanostructures is the phenalenyl radical, which is obtained by single deprotonation of the phenalene molecule. Similar to many other related and extensively studied structures [10–12], this radical is stable and displays a net magnetic moment of 1 μ_B [13–20]. Phenalenyl radicals may polymerize and form a 2D “nanoporous graphene” metamaterial that may be deformed by strain to display a complex behavior of the Poisson’s ratio including strain-related changes in value and sign [1]. Strain-related changes in coupling between connected phenalenyl radicals, which carry a nonvanishing magnetic moment, may change not only the electronic structure of the system, but also its magnetic order. Elemental substitution of carbon by boron or nitrogen in the radicals may cause additional drastic changes in the magnetic behavior.

Here, we report the design of a Kagomé-like 2D metamaterial, which is composed of phenalenyl radicals covalently interconnected at their corners. This pristine metamaterial exhibits a strong ferromagnetic order, which can be tuned significantly by applied strain at little energy cost. In this metamaterial, externally applied strain primarily turns the phenalenyl radicals with respect to each other. We find that this deformation, which changes the magnetic moment of individual radicals, is accompanied by a charge flow that may change the system from a metal to a narrow-gap semiconductor. Substitutional doping of this metamaterial, caused by replacing carbon by either boron or nitrogen atoms, decreases the net magnetization significantly. However, simultaneous doping by B and N changes the magnetic order to antiferromagnetic. Unlike in the pristine system, strain-induced turning of the doped phenalenyl radicals does not change their magnetic moment. The structures described here are constrained to planar geometries during deformation, which can be realized by being attracted to a planar substrate or in a sandwich geometry.

* Corresponding author.
E-mail address: tomanek@msu.edu (D. Tománek).

https://doi.org/10.1016/j.carbon.2020.01.053
0008-6223/

2. Results

2.1. Kagomé-like 2D polyphenalenyl as magnetic metamaterial

The optimized phenalenyl radical, also called perinaphthenyl, obtained by mono-deprotonation of the phenalene molecule and shown in Fig. 1 (a), is composed of 13 carbon and 9 hydrogen atoms ($C_{13}H_9$). Since the phenalenyl radical is missing one H compared to the non-magnetic phenalene, it carries one unpaired electron, resulting in a net magnetic moment of 1 μ_B. Within the Hückel molecular approximation, the non-bonding singly-occupied molecular orbital (SOMO) of $C_{13}H_9$ locates the spin density in a uniform and regular fashion on every other of the 12 equivalent peripherical conjugated carbon atoms [21]. The macroscale 2D metamaterial polyphenalenyl, shown in Fig. 1(b), is an optimized structure of polymerized phenalenyl radicals that are covalently connected at the corners. There are two identical phenalenyl radicals with different orientation in the primitive unit cell of polyphenalenyl, as seen in Fig. 1(b). To provide for increased freedom in the magnetic order, we choose a unit cell that is rectangular and twice as large as the primitive unit cell.

To save computer time when considering many 2D polyphenalenyl metamaterials with different relative orientation angles β, we first optimized the connection distance between frozen phenalenyl radicals and then relaxed the hydrogen atoms while keeping the carbon atoms frozen. We refer to this optimization strategy as 'partial global relaxation' in the discussion hereafter. Compared to a more accurate and time-consuming global relaxation, structures optimized in this way were found to be less stable by only $\lesssim$21 meV/C-atom with respect to globally optimized structures. We found also only small differences of $\lesssim$0.6% between structures optimized globally or in the simplified way. We concluded that the geometry and stability of globally optimized structures are reproduced very well by partial global relaxation and used the latter approach to optimize all geometries in this study unless stated otherwise. We find energetic preference for ferromagnetic ordering in the optimized 2D metamaterial. The calculated magnetic moment of one unit cell, which contains four radicals, is $\approx$3.6 μ_B. We found all phenalenyl radicals in the unit cell to carry the same magnetic moment of 0.9 μ_B, which is somewhat smaller than the 1 μ_B value of an isolated phenalenyl radical and is a consequence of polymerization.

Under compressive strain, deformed structures can be characterized by the angle β, defined in Fig. 1(b), which describes the relative orientation of adjacent radicals. $\beta = 120^\circ$ in the optimized structure of 2D polyphenalenyl. β may increase or decrease under in-plane compressive strain, but will not change under tension. The deformation energy ΔE depends on the deformation characterized by the angle β. As seen in Fig. 1(c), ΔE exhibits a harmonic change around the equilibrium value $\beta = 120^\circ$. We find that changing β by 20° requires 5 eV per unit cell or 96 meV/C-atom, which is only $\approx$2% of the bond strength. This means this 2D polyphenalenyl is a soft metamaterial that can be deformed easily by applying in-plane stress.

Changing β by in-plane compression causes a net charge flow in the structure. We first study the charge flow in a dimer made of two phenalenyl radicals connected by one C–C bond, shown in Fig. 2(a) for $\beta = 100^\circ$. Decreasing β from the equilibrium value, we find that more electrons accumulate at the edges that are approaching during the deformation, and deplete at the edges that are getting more distant. Even though the net charge and net magnetic moment of 2 μ_B of the system remain the same, the local charge density and the local magnetic moment may change as *beta* changes. We characterize the difference between the sum of local magnetic moments in atoms on the upper and lower edges of one of the radicals by the quantity ΔM. As we show in Fig. 2(b), ΔM increases monotonically along with charge density differences as β deviates from the equilibrium value of 120°.

Unlike in the dimer discussed above, each phenalenyl radical is connected not to one, but three radicals in 2D polyphenalenyl, as

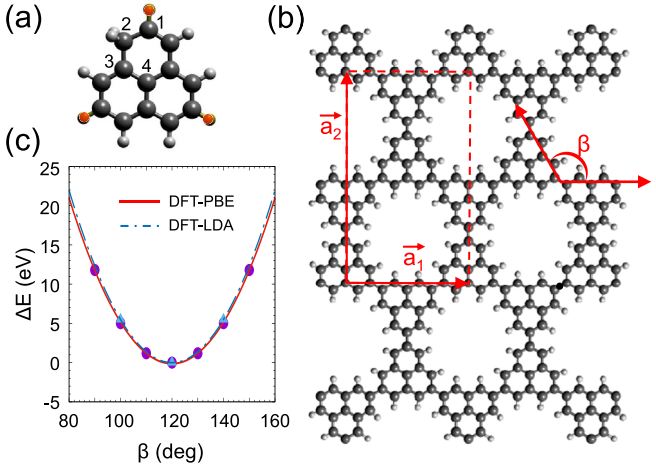

Fig. 1. Polymerization of phenalenyl radical units into a Kagomé-like 2D polyphenalenyl lattice. (a) Phenalene (1*H*-Phenalene, $C_{13}H_{10}$), a polycyclic aromatic hydrocarbon (PAH), used to produce the phenalenyl radical by deprotonation of one of the corner atoms. (b)$(C_{13}H_6)_\infty$ polyphenalenyl lattice. The primitive unit cell is delimited by the lattice vectors $\vec{a}_1$ and $\vec{a}_2$. The three hydrogens in phenalene, highlighted in (a), detach when forming polyphenalenyl. (c) Total energy change ΔE per unit cell caused by the changing orientation angle β, obtained using DFT-PBE (red solid line) and DFT-LDA (blue dashed line). (A colour version of this figure can be viewed online.)

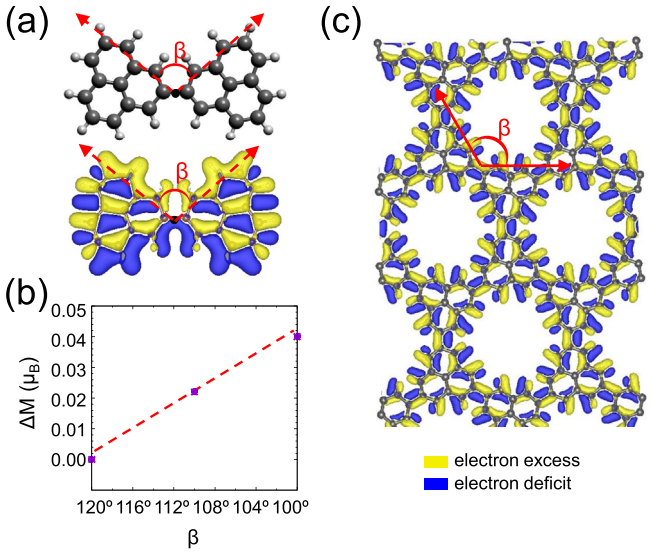

Fig. 2. (a) Top view of the deformed phenalenyl dimer $C_{26}H_{18}$ with $\beta = 100^\circ$ in the upper panel. Charge redistribution in the phenalenyl dimer caused by deviation from the equilibrium structure with $\beta = 120^\circ$ is shown in the lower panel, which depicts isosurface bounding regions of electron excess at $+3.2 \times 10^{-2}$ e/Å^3 (yellow) and electron deficiency at -3.2×10^{-2} e/Å^3 (blue). (b) Difference between the relative contribution of the upper and lower atoms towards the net magnetic moment $M = 2\ \mu_B$, presented as a function of the relative orientation angle β in the phenalenyl dimer $C_{26}H_{18}$. (c) Charge redistribution in strained polyphenalenyl with $\beta = 100^\circ$, caused by deviation from the equilibrium structure with $\beta = 120^\circ$. (A colour version of this figure can be viewed online.)

seen in Fig. 2(c). As individual radicals rotate in an alternate way during deformation, each edge of any radical approaches and distances itself from edges of two adjacent radicals, compensating for the charge flow from the two sides. There is no net charge accumulation on any of the edges, but still a local charge redistribution within each radical. This changes the electronic structure and magnetic behavior of the 2D polyphenalenyl system.

2.2. Strain-controlled electronic and magnetic properties of the Kagomé-like 2D polyphenalenyl metamaterial

As mentioned above, deformation of the 2D polyphenalenyl structure under in-plane compressive strain can be characterized by changes in the orientation angle β. Under uniform in-plane tensile strain, $\beta = 120^\circ$ does not change and there is only an increase in the C–C bond length. The deformation energy as a function of in-plane strain is shown in Fig. 3(a). Results provided for the $\varepsilon < 0$ range in this figure correspond to those for β deviating from the 120° equilibrium value in Fig. 1(c). Our results for $\varepsilon > 0$ indicate that the systems is rather soft also under tension, since 1% tensile strain requires an energy investment of only $\Delta E < 1$ eV per unit cell.

Lattice deformation also affects the electronic and thus the magnetic structure of the system. As seen in Fig. 3(b), the magnetic moment per unit cell M is particularly sensitive to compressive strain that changes the angle β. In comparison to $M = 3.6\ \mu_B$ in the unstrained lattice, the magnetic moment reduction to $M = 0.1\ \mu_B$ under $\varepsilon = -0.12\%$ compression is significant. We find the magnetic moment to increase less rapidly under tension, achieving $M = 4.0\ \mu_B$ at $\varepsilon = +1.0\%$ due to reduced coupling between the phenalenyl radicals.

The magnetic behavior of the system under strain is shown in the spin-polarized DOS in Fig. 3(c). There is a majority band (spin-up) that overlaps partly with the minority band (spin-down), rendering the system metallic under zero or compressive strain. It is this increasing band overlap that is responsible for quenching the magnetic moment under increasing compressive strain. Increasing tensile strain beyond $\varepsilon \gtrsim 0.5\%$ opens a narrow semiconducting gap between the majority and minority bands and the magnetic moment saturates at $M = 4.0\ \mu_B$. The system remains ferromagnetic in the entire deformation range discussed here.

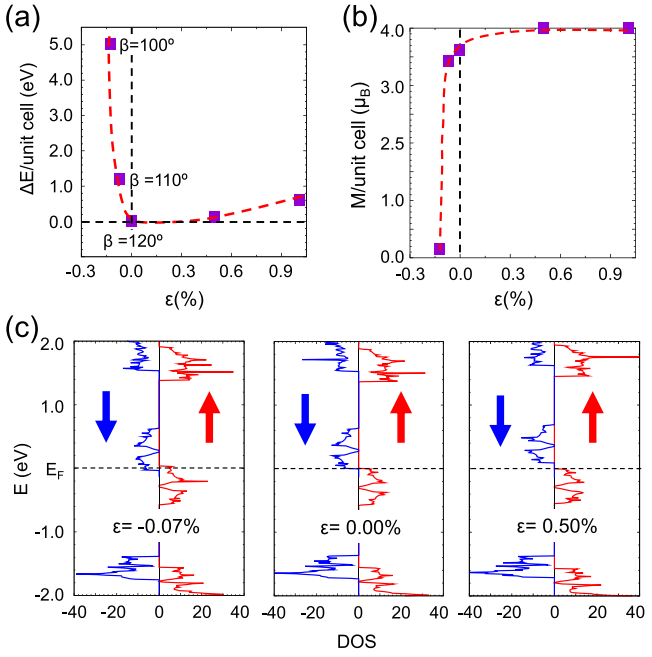

Fig. 3. Strain-dependent properties of the Kagomé-like 2D polyphenalenyl metamaterial. (a) Deformation energy ΔE as a function of in-plan strain ε. (b) Total magnetic moment M per unit cell as a function of ε. (c) Spin-polarized density of states (DOS) for different values of ε. The different spin polarizations are distinguished by color. (A colour version of this figure can be viewed online.)

2.3. Adsorption of phenalenyl radicals on graphene and h – BN

Clearly, the Kagomé-like 2D polyphenalenyl system needs to be stabilized by a substrate against structural collapse. An ideal substrate should be stable and capable of supporting the Kagomé-like 2D lattice, but should not affect its electronic and magnetic structure. We have considered monolayers of graphene and hexagonal boron nitride (h – BN) as suitable substrates that are both stable and chemically non-reactive.

The adsorption geometry of $C_{13}H_9$ radicals on graphene and h – BN is shown for one unit cell of a superlattice in Fig. 4(a–b). We find the equilibrium separation between phenalenyl and the substrate to be $h = 4.0$ Å for graphene and $h = 3.9$ Å for h – BN. These separations are similar to the interlayer distance of graphite and h – BN.

The DFT-based energy level spectrum of an isolated $C_{13}H_9$ radical is presented in Fig. 4(c). We expect the weak interaction between $C_{13}H_9$ and the substrate not to affect its electronic structure much. To quantify this effect, we present ΔDOS as the difference between the DOS of the combined system and the superposition of densities of states of the isolated radicals and the isolated substrate in Fig. 4(d) for graphene and Fig. 4(e) for h – BN. As expected, we find ΔDOS very small in comparison to the DOS of polyphenalenyl in Fig. 3(c). Consequently, the effect of adsorbate-substrate interaction on the electronic and related magnetic structure of phenalenyl can be neglected. In that case, results for a free-standing Kagomé-like 2D polyphenalenyl system should apply also in presence of substrates such as graphene and h – BN, or in a sandwich geometry between such layers. Preventing polymerization due to collapse of the 2D polyphenalenyl monolayer or by

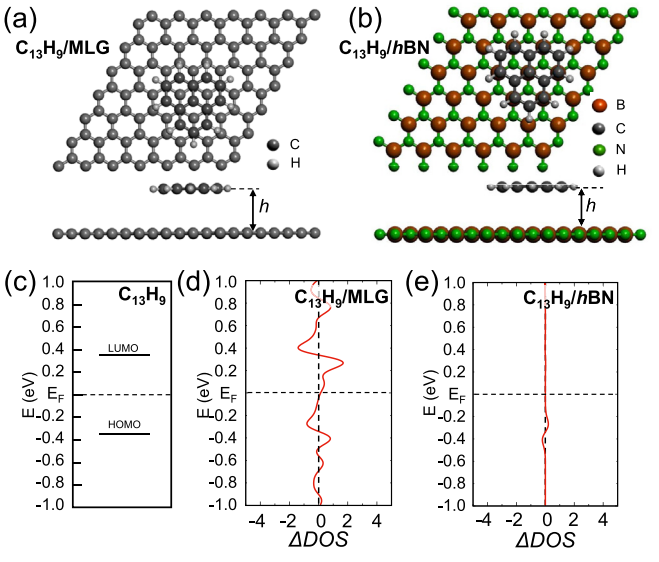

Fig. 4. Equilibrium structure and adsorption-induced changes in the DOS of $C_{13}H_9$ adsorbed on graphene and h – BN. Top and side views of the adsorption geometry of $C_{13}H_9$ on (a) graphene and (b) h – BN substrates. (c) The DFT energy level spectrum of a $C_{13}H_9$ molecule. Adsorption-induced changes in the DOS of phenalenyl on (d) graphene and (e) h – BN, with $\Delta DOS = DOS(C_{13}H_9/\text{substrate}) - DOS(C_{13}H_9) - DOS(\text{substrate})$. All results are based on superlattice calculations. (A colour version of this figure can be viewed online.)

allowing multilayer formation is a key to maintaining the intriguing magnetic behavior described here.

2.4. Effect of doping on magnetic properties of strained Kagomé-like 2D polyphenalenyl

As mentioned above, the phenalenyl radical $C_{13}H_9$ carries the magnetic moment 1 μ_B due to one unpaired electron in the radical. Replacing a carbon atom in the phenalenyl radical by boron with one less valence electron or by nitrogen with one more valence electron will change the charge of the radical by one, allowing all electrons to pair. Consequently, doped phenalenyl radicals $C_{12}BH_9$ and $C_{12}NH_9$ should be non-magnetic. In the phenalenyl radical displayed in Fig. 1(a), we can distinguish four inequivalent carbon sites, labeled $1-4$, among the 13 carbon atoms in total. Replacing any of these 4 C atoms by B or N quenched the magnetic moment of the doped radical to zero as suggested above.

Optimum location of the dopant atoms within the 2D metamaterial is driven by stability considerations. As a guiding principle, we compared the bond strength of C—C, B—N, C—B and C—N dimers. Among these, the C—C bond was most stable, followed by the 1.9 eV less stable B—N bond. The C—N bond was found to be almost as stable as the B—N bond, and the C—B bond was found to be 2.8 eV less stable than the B—N bond. Based on these findings, a stable 2D metamaterial allotrope may consist of phenalenyl radical pairs connected by B—N instead of C—C bonds, as seen in Fig. 5(a).

The $(C_{12}H_6B-C_{12}H_6N)_\infty$ 2D polyphenalenyl lattice doped with B and N atoms, shown in Fig. 5(a), carries zero magnetization, as illustrated by the symmetric spin-polarized DOS in Fig. 5(b). In contrast to the pristine metamaterial which is a metal, the doped metamaterial is a semiconductor with a narrow band gap of about 0.06 eV seen in Fig. 5(b).

The spin-polarized charge density $\rho_\uparrow - \rho_\downarrow$ of the doped polyphenalenyl lattice is shown in Fig. 5(c), with the two spin polarizations being distinguished by color. We clearly see that the dominant color on the B-doped phenalenyl radical is red, indicating a majority state with spin-up electrons and a net magnetic moment of $\approx 0.35\ \mu_B$. The dominant color on the N-doped phenalenyl radical is dark blue, indicating that the majority state carries spin-down electrons and a net magnetic moment of $\approx -0.35\ \mu_B$. This is somewhat unexpected, since separated doped radicals were found to be non-magnetic, and indicates the role of coupling and charge transfer between connected radicals. With magnetic moments of opposite direction on adjacent phenalenyl radicals in the unit cell, the 2D metamaterial is antiferromagnetic.

Same as in the pristine metamaterial, in-plane compressive strain changes the orientational angle β of the doped phenalenyl radicals. In B—N doped polyphenalenyl, changing β by 20° from the equilibrium value requires an energy investment of 4.46 eV/unit cell, slightly less than in the pristine system according to Fig. 3(a). As we showed in Fig. 3(b), even minute compressive strain that changed β by 20° caused a significant reduction of the magnetic moment in the pristine system. In the B—N doped system, on the other hand, the same change of β by 20° has very little effect on the local magnetization of B- and N-doped phenalenyl radicals. Even under in-plane compressive strain, the doped 2D polyphenalenyl remains a narrow-gap semiconductor and anti-ferromagnet. Additional results depicting changes in the spin-polarized charge density of pristine and doped polyphenalenyl caused by changes in β are presented in the Supporting Material [22].

The 2D metamaterial composed of $C_{13}H_9$ phenalenyl radicals carrying a 1 μ_B magnetic moment is just one member of a large family of polycyclic aromatic hydrocarbons (PAHs). Other PAH molecules or radicals have different magnetic properties, including the non-magnetic $C_{14}H_{10}$ phenanthrene molecule considered as component of a 'mechanical' metamaterial described in Ref. [1]. When substitutionally doped with B or N, also this molecule should carry a 1 μ_B magnetic moment according to Hund's rule. Consequently, a 2D metamaterial consisting of polymerized pristine $C_{14}H_{10}$ molecules should be non-magnetic. Doping every other molecule by boron and the remaining molecules by nitrogen, polyphenanthrene may acquire interesting magnetic behavior. The effect of B or N doping in polyphenalenyl and polyphenanthrene is thus opposite. With specific applications in mind, other PAH molecules can be chosen as building blocks of 2D metamaterials.

We have seen that doping every other phenalenyl radical in polyphenalenyl by B and the remaining radicals by N has changed the magnetic order from ferromagnetic in the pristine system to antiferromagnetic in the doped metamaterial. The cause underlying this change was the charge transfer in the polar B—N links connecting the radicals. There are other methods to modify the charge distribution in 2D systems including a 'van der Waals' 2D/2D contact with a substance like the Ca_2N electride, which has been shown to transfer a significant charge to systems such as 2D boron [23]. In the rigid-band model, electron transfer to B—N doped polyphenalenyl would raise the Fermi level and fill initially empty spin-up and spin-down bands to a different degree, leading to a nonzero global magnetization. Since B-doped and N-doped phenalenyl radicals carry opposite net charges causing opposite magnetic moments, uniform electron doping would break this symmetry in charge doping and magnetic moments, turning the system ferrimagnetic.

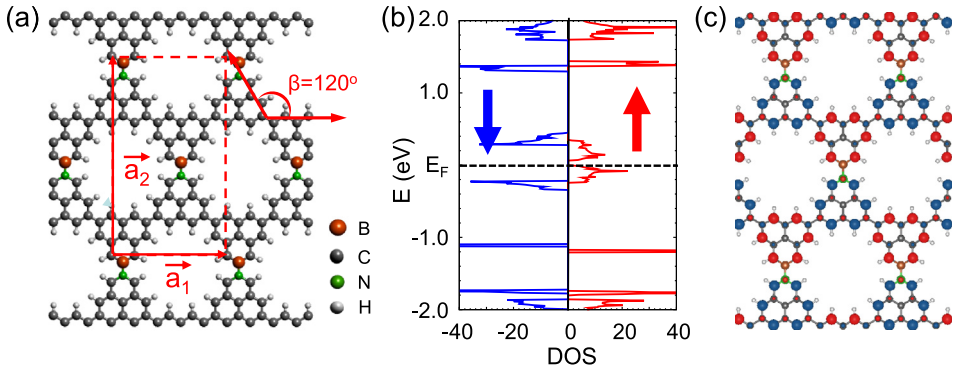

Fig. 5. Kagomé-like $(C_{12}H_6B-C_{12}H_6N)_\infty$ 2D polyphenalenyl lattice doped with B and N atoms. (a) Top view of the equilibrium lattice structure with $\beta = 120°$. The conventional unit cell, delimited by the $\vec{a}_1$ and $\vec{a}_2$ basis vectors, contains two formula units. (b) Spin-polarized DOS of the doped polyphenalenyl lattice shown in panel (b). Spin-up and spin-down DOS are distinguished by color. (c) Spin polarized charge density $\rho_\uparrow - \rho_\downarrow$ in the B—N doped 2D polyphenalenyl lattice of panel (a). The isosurfaces are bounded by $+2\times 10^{-3}$ e/Å^3 for the ↑ spin (red) and by -2×10^{-3} e/Å^3 for the ↓ spin (dark blue). (A colour version of this figure can be viewed online.)

3. Summary and conclusions

We have used *ab initio* spin-polarized DFT calculations to study the magnetic order in a Kagomé-like 2D metamaterial consisting of pristine or substitutionally doped phenalenyl radicals polymerized into a nanoporous, graphene-like structure. In this and in a larger class of related structures, the constituent PAH molecules can be considered as quantum dots that may carry a net magnetic moment. The structure of this porous system is rather soft and may be changed at little energy cost by applying in-layer strain. Structural changes modify the coupling between such quantum dots, causing a change in the electronic and magnetic structure. The pristine polyphenalenyl material is ferromagnetic, but its magnetization may be changed by a factor of two by applying moderate strain. Doping every other radical by B or N atoms turns the system antiferromagnetic, with local magnetic moments rather independent of strain-related structural changes. We believe this is only one interesting example of how to control the magnetic order and the underlying electronic structure in magnetic metamaterials.

4. Computational techniques

We have studied the electronic and magnetic properties as well as the deformation energy of polyphenalenyl using *ab initio* density functional theory (DFT) as implemented in the VASP code [24–26]. We represented this 2D structure by imposing periodic boundary conditions in all directions and separating individual layers by a vacuum region of 15 Å. We used projector-augmented-wave (PAW) pseudopotentials [27,28] and the Perdew-Burke-Ernzerhof (PBE) [29] or the Local Density Approximation (LDA) [30,31] exchange-correlation functionals. The Brillouin zone of the conventional unit cell of the 2D structure was sampled by an $11\times 5\times 1$ *k*-point grid [32]. We used a value of 500 eV as the electronic kinetic energy cutoff for the plane-wave basis and a total energy difference between subsequent self-consistency iterations below 10^{-4} eV as the criterion for reaching self-consistency. All geometries have been optimized using the conjugate-gradient method [33], until none of the residual Hellmann-Feynman forces exceeded 10^{-2} eV/Å.

Acknowledgments

D.L. and D.T. acknowledge financial support by the NSF/AFOSR EFRI 2-DARE grant number EFMA-1433459. Computational resources have been provided by the Michigan State University High Performance Computing Center. Sandia National Laboratories is a multi-mission laboratory managed and operated by National Technology and Engineering Solutions of Sandia, LLC., a wholly owned subsidiary of Honeywell International, Inc., for the U.S. Department of Energy's National Nuclear Security Administration under Contract DE-NA0003525. The views expressed in the article do not necessarily represent the views of the U.S. DOE or the United States Government.

Appendix A. Supplementary data

Supplementary data to this article can be found online at https://doi.org/10.1016/j.carbon.2020.01.053.

References

[1] Z. Gao, D. Liu, D. Tománek, Two-dimensional mechanical metamaterials with unusual Poisson ratio behavior, Phys. Rev. Appl. 10 (2018), 064039.
[2] G. Scalari, C. Maissen, D. Turčinková, D. Hagenmüller, S. De Liberato, C. Ciuti, C. Reichl, D. Schuh, W. Wegscheider, M. Beck, J. Faist, Ultrastrong coupling of the cyclotron transition of a 2D electron gas to a THz metamaterial, Science 335 (6074) (2012) 1323–1326.
[3] B.D.F. Casse, H.O. Moser, L.K. Jian, M. Bahou, O. Wilhelmi, B.T. Saw, P.D. Gu, Fabrication of 2D and 3D electromagnetic metamaterials for the terahertz range, J. Phys. Conf. Ser. 34 (2006) 885–890.
[4] A. Ishikawa, S. Hara, T. Tanaka, X. Zhang, K. Tsuruta, Robust plasmonic hotspots in a metamaterial lattice for enhanced sensitivity of infrared molecular detection, Appl. Phys. Lett. 111 (24) (2017) 243106.
[5] M. Treier, C.A. Pignedoli, T. Laino, R. Rieger, K. Müllen, D. Passerone, R. Fasel, Surface-assisted cyclodehydrogenation provides a synthetic route towards easily processable and chemically tailored nanographenes, Nat. Chem. 3 (1) (2011) 61.
[6] C. Moreno, M. Vilas-Varela, B. Kretz, A. Garcia-Lekue, M.V. Costache, M. Paradinas, M. Panighel, G. Ceballos, S.O. Valenzuela, D. Peña, A. Mugarza, Bottom-up synthesis of multifunctional nanoporous graphene, Science 360 (6385) (2018) 199–203.
[7] M. Bieri, M. Treier, J. Cai, K. Ait-Mansour, P. Ruffieux, O. Groning, P. Groning, M. Kastler, R. Rieger, X. Feng, K. Müllen, R. Fasel, Porous graphenes: two-dimensional polymer synthesis with atomic precision, Chem. Commun. 45 (2009) 6919–6921.
[8] P. Xu, J. Yang, K. Wang, Z. Zhou, P. Shen, Porous graphene: properties, preparation, and potential applications, Chin. Sci. Bull. 57 (23) (2012) 2948–2955.
[9] M.E. Khan, P. Zhang, Y.-Y. Sun, S.B. Zhang, Y.-H. Kim, Tailoring graphene magnetism by zigzag triangular holes: a first-principles thermodynamics study, AIP Adv. 6 (3) (2016), 035023.
[10] M. Nakano, R. Kishi, S. Ohta, H. Takahashi, T. Kubo, K. Kamada, K. Ohta, E. Botek, B. Champagne, Relationship between third-order nonlinear optical properties and magnetic interactions in open-shell systems: a new paradigm for nonlinear optics, Phys. Rev. Lett. 99 (2007), 033001.
[11] A. Konishi, Y. Hirao, M. Nakano, A. Shimizu, E. Botek, B. Champagne, D. Shiomi, K. Sato, T. Takui, K. Matsumoto, H. Kurata, T. Kubo, Synthesis and characterization of teranthene: a singlet biradical polycyclic aromatic hydrocarbon having Kekulé structures, J. Am. Chem. Soc. 132 (32) (2010) 11021–11023.
[12] T. Kubo, A. Shimizu, M. Sakamoto, M. Uruichi, K. Yakushi, M. Nakano, D. Shiomi, K. Sato, T. Takui, Y. Morita, K. Nakasuji, Synthesis, intermolecular interaction, and semiconductive behavior of a delocalized singlet biradical hydrocarbon, Angew. Chem. Int. Ed. 44 (40) (2005) 6564–6568.
[13] P.B. Sogo, M. Nakazaki, M. Calvin, Free radical from perinaphthene, J. Chem. Phys. 26 (5) (1957) 1343–1345.
[14] E. de Boer, Hyperfine structure and electron densities in aromatic free radicals, J. Chem. Phys. 25 (1) (1956), 190–190.
[15] H.M. McConnell, D.B. Chesnut, Negative spin densities in aromatic radicals, J. Chem. Phys. 27 (4) (1957) 984–985.
[16] H.M. McConnell, H.H. Dearman, Spin densities in the perinaphthenyl free radical, J. Chem. Phys. 28 (1) (1958) 51–53.
[17] D. Reid, Stable π-electron systems and new aromatic structures, Tetrahedron 3 (3) (1958) 339–352.
[18] F. Gerson, Notiz über das ESR-Spektrum des Phenalenyl-Radikals, Helv. Chim. Acta 49 (5) (1966) 1463–1467.
[19] R.C. Haddon, F. Wudl, M.L. Kaplan, J.H. Marshall, R.E. Cais, F.B. Bramwell, 1,9-dithiophenalenyl system, J. Am. Chem. Soc. 100 (24) (1978) 7629–7633.
[20] K. Uchida, T. Kubo, Recent advances in the chemistry of phenalenyl, J. Syn. Org. Chem. Jpn 74 (11) (2016) 1069–1077.
[21] G. Trinquier, J.-P. Malrieu, Spreading out spin density in polyphenalenyl radicals, Phys. Chem. Chem. Phys. 19 (2017) 27623–27642.
[22] See the Supplemental Material at https://doi.org/10.1016/j.carbon.2020.01.053 for Results Depicting Changes in the Spin-Polarized Charge Density of Pristine and Doped 2D Polyphenalenyl Caused by In-Layer Compressive Strain.
[23] D. Liu, D. Tománek, Effect of net charge on the relative stability of 2D boron allotropes, Nano Lett. 19 (2) (2019) 1359–1365.
[24] G. Kresse, J. Furthmüller, Efficient iterative schemes for ab initio total-energy calculations using a plane-wave basis set, Phys. Rev. B 54 (1996) 11169–11186.
[25] G. Kresse, J. Furthmüller, Efficiency of ab-initio total energy calculations for metals and semiconductors using a plane-wave basis set, Comput. Mater. Sci. 6 (1) (1996) 15–50.
[26] G. Kresse, J. Hafner, *Ab initio* molecular-dynamics simulation of the liquid-metal–amorphous-semiconductor transition in germanium, Phys. Rev. B 49 (1994) 14251–14269.
[27] P.E. Blöchl, Projector augmented-wave method, Phys. Rev. B 50 (1994) 17953–17979.
[28] G. Kresse, D. Joubert, From ultrasoft pseudopotentials to the projector augmented-wave method, Phys. Rev. B 59 (1999) 1758–1775.
[29] J.P. Perdew, K. Burke, M. Ernzerhof, Generalized gradient approximation made simple, Phys. Rev. Lett. 77 (1996) 3865–3868.
[30] D.M. Ceperley, B.J. Alder, Ground state of the electron gas by a stochastic method, Phys. Rev. Lett. 45 (1980) 566–569.
[31] J.P. Perdew, A. Zunger, Self-interaction correction to density-functional approximations for many-electron systems, Phys. Rev. B 23 (1981) 5048–5079.
[32] H.J. Monkhorst, J.D. Pack, Special points for Brillouin-zone integrations, Phys. Rev. B 13 (1976) 5188–5192.
[33] M.R. Hestenes, E. Stiefel, Methods of conjugate gradients for solving linear systems, J. Res. Natl. Bur. Stand. 49 (1952) 409–436.